# COMPOSITE INFLATABLE ANTENNAS FOR SMALL – SATELLITES AND BACKUP COMMUNICATION

Aman Chandra
Department of Aerospace and Mechanical Engineering,
University of Arizona, 1130 N Mountain Ave, Tucson, Arizona, achandra@email.arizona.edu

Jekanthan Thangavelautham
Department of Aerospace and Mechanical Engineering,
University of Arizona, 1130 N Mountain Ave, Tucson, Arizona, jthanga@email.arizona.edu

Alessandra Babuscia
Jet Propulsion Laboratory, 4800 Oak Grove Dr, Alessandra.Babuscia@jpl.nasa.gov

## Abstract

There is an ever-growing need for deployment of large space structures with large apertures for applications such as communication relays. There is also rapid growth in small spacecraft such as CubeSats and Small-Sats for deep space science missions but are limited by their size and how much they can communicate back to Earth. In addition, there is a growing need to have backup communication systems on large satellites that will have minimal mass, volume and power footprint. There are several competing technologies for deployment of space structures such as interlinked deployable mechanisms and inflatables. Interlinked deployable mechanisms contain mechanisms with many hundreds of moving parts that dependent on each-other for successful deployment. Inflatables are relatively simple and offer the best stowage and mass footprint. They can use green (non-toxic) sublimates to inflate and be rigidized using UV curing. These inflatables offer the highest volume to mass stowage ratios, while providing a rigid product in space. The system is also puncture resistant to micro-meteorites. However, challenges remain with composite inflatable in achieving high-quality finished surface required for a x-band or Ka-band communication antenna. Our work is focusing on composite inflatables that combines different materials, such as inflatables containing modular bladders with soft and rigid materials, miniature sensors and actuators to form a structure. Composite inflatables are born out of the size, rigidity limitations and precision limitations of conventional inflatables. The advantage of a composite inflatable is it is modular, smart, has strength and rigidity properties of a solid, but is mostly gas. Each module can be independently adjusted to fine-tune the overall shape and perform corrections to varying environmental conditions. Our research is focused on developing Ka-band inflatable antenna for CubeSats that range in size from 1 to 3 m and can be stowed in a 1 to 1.5 U package. The technology will utilize composite inflatables that produce a smooth wrinkle free surface, a parabolic shape, modular structure to withstand local punctures and sufficient rigidity under varying in-space conditions. Inflatables offer the lowest mass, lowest stowage volume design yet. Our studies have shown inflatable achieving up to a 10-fold mass and volume savings compared to conventional structures. Advancement of this technology offers advantage in producing ultra-low cost communication constellation satellites. Our work combines use of analytical tools, high-fidelity simulations with laboratory experiments and demonstrations in a thermal vacuum chamber. In this work, we will for the first time apply analytical structural design principles and high-fidelity structural simulation tools to show how a composite inflatable for Ka-band antenna will take shape. This will be complemented with simulations of the resultant antenna radiation pattern. Our work will then proceed to outline plans for laboratory development and testing of a 2-m Ka-inflatable antenna.

## Introduction

Small satellites such as CubeSats hold the potential to significantly reduce the cost of space exploration. CubeSats [1] allow commercial off the shelf (COTS) components to be integrated reliably and efficiently. This renders CubeSats to be relatively low-cost means to access space. While traditionally limited to lower earth orbits (LEO), improvements in electronics miniaturization and control [2] have facilitated more complex deep space missions using CubeSats. Specified to standard sizes, CubeSats are constrained by limited available payload mass and volume. This imposes great restrictions on the size of any instrument on-board the spacecraft. A direct consequence of this is a limitation on the types of available sensors and equipment that can be integrated within CubeSats.

Current CubeSat antenna technologies do not provide sufficient data downlink rates for efficient high quality data transfer. This is further reduced for CubeSats in deeper space and interplanetary orbits. A limited communications capability is one of the biggest challenges facing small satellite technology. To enhance antenna radiative power, higher frequency bandwidths are considered ideal. The efficient utilization of high frequency communication bandwidths of 20 Ghz and above require high gain narrow beam-width antennas. These antennas additionally provide low side lobe levels which is also a desirable [3] for directive radiation patterns. This leads us to a class of antennas termed as high gain antennas (HGA's) with highly directive radiation patterns. Figure 1 illustrates the MarCO CubeSat mission to Mars acting as an example of a CubeSat based HGA for interplanetary telecommunication.

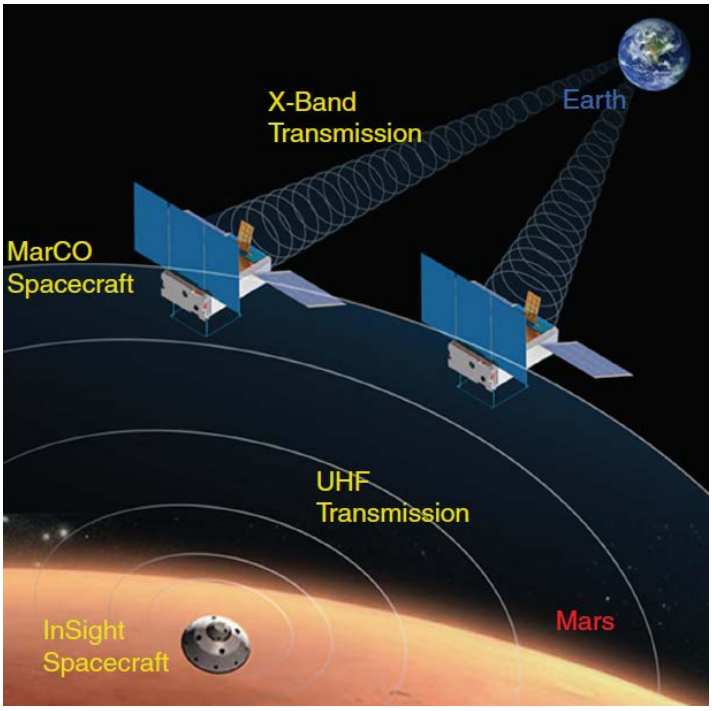


Figure 1. MarCO Mars to Earth HGA telecom relay [4]

HGA technologies in operation include lens antennas, reflect-arrays and reflectors. A common requirement from all of these technologies is a high aperture cross section. A larger cross sectional area is desired to achieve high gain requirements. To be compatible with the CubeSat form factor, the HGA of choice would be one with a high deployed surface area to stowed volume ratio. Additional requirements include a structurally reliable and accurate feed structure. Table 1 compares various HGA technologies suitable for CubeSats.

Table 1. Comparison of HGA technologies for CubeSats

| HGA technology | Aperture ($cm^2$) | Gain (Ka-Band) (dB) | Bandwidth | Side-lobe levels |
|---|---|---|---|---|
| Lens antennas | 600 - 1000 | 18 – 24 | Medium | Low |
| Reflect-arrays | 1000 - 2000 | >28 | Medium | Low |
| Reflectors | 1500 - 2000 | >28 | Large | Medium |

From the table, it can be seen that reflector offer the highest gain and bandwidth. Our present work focuses on reflector antennas in the Ka-Band. Traditional reflectors have exhibited complex structural deployment involving mechanisms and moving parts. This leads to low-reliability and a reduced ability to scale to large sizes. Our research looks into means of creating a CubeSat-based deployable reflector with the ability to be enlarged several meters in size. Among the reflector technologies developed, inflatables hold the most promise. Table 2 summarizes deployable reflector technologies that have been developed.

Table 2. Comparison of CubeSat Reflector technologies

| Reflector technology | Deployment Complexity | Packing Efficiency | Mass/ unit surface area | Scalability |
|---|---|---|---|---|
| Fixed reflectors | Low | 1:1 | 1-2 kg | Low |
| Deployable reflectors | High | 5:1 | 1-2 kg | Medium |
| Inflatable reflectors | Low | 20:1 | 0.3 – 0.5 kg | High |

It is evident that inflatables offer the greatest promise with respect to compaction efficiency, low mass and volume. The absence of moving parts or mechanisms also make this technology highly scalable. This has motivated development of an inflatable antenna prototype. In the present work, we build upon our previous work on inflatables. We set out to characterize the geometric and communications performance of the developed inflatable reflector element. We look at the problem from a structural reliability point of view to understand how surface characteristics can be improved to achieve high-gain CubeSat reflectors. Desired structural traits identified are then used to propose more complex inflatable assemblies that could potentially lead to significant improvements in surface characteristics required by high gain antennas.

## Related Work

The first large scale inflatables used for communication were in the echo balloon project by NASA in the 1960's [5]. Two satellites, the ECHO 1 and 2 were large orbiting spheres constructed out of metallized Mylar membrane that were 30 meters in diameter. Both missions served as passive reflectors for ground station signals operating in the frequency range of 162 to 2390 MHz. Ground antennas required large transmit powers in the 10 kW range. ECHO 1 and 2 remained in orbit for 8 and 5 years respectively. This validated inflatable technology as a robust technology for Low Earth Orbit conditions.

The success of the ECHO mission triggered investigation into more complex inflatable concepts. Since the 1970's, L'Garde Inc. developed inflatable antennas up to several meters in diameter. This work later formed

the basis of the inflatable antenna experiment in the late 1990's. A 16-meter diameter reflective parabola was deployed on board STS 77 (Space Shuttle) and demonstrated successful deployment in LEO [6]. The primary objectives of the mission were to understand dynamic characteristics of deployment. RF measurements were not performed. Figure 2 shows an image of the experiment in deployed state.

A parallel effort towards developing rigidized parabolas was performed by the Contraves Space Division in Switzerland in collaboration from ESA [7]. Resin impregnated Kevlar was used as backing to construct parabolic reflectors of up-to 12 m in diameter. The resin enabled hardening of the structure in about 3 hours post deployment. Ground based tests showed impressive surface characteristics. The structure, however, was not tested as a deployable system in space.

Major hurdles towards realizing a truly reliable inflatable antenna system have been the lack of simulation and modelling techniques to design deployable structures [8]. Complex geometric interactions between stowed states of membranes as compared to their final inflated structures lead to approximate estimates of the design's performance usually not considered reliable enough for high risk space missions.

Prior work on inflatables brings us to understand that a feasible inflatable reflector system would need a deployment device that's mechanically simple. Another requirement would be the ability of the inflatable system to be activated using passive chemical processes. Finally, the inflatable would need to be rigidized to withstand micrometeorites, dust and debris particles in space.

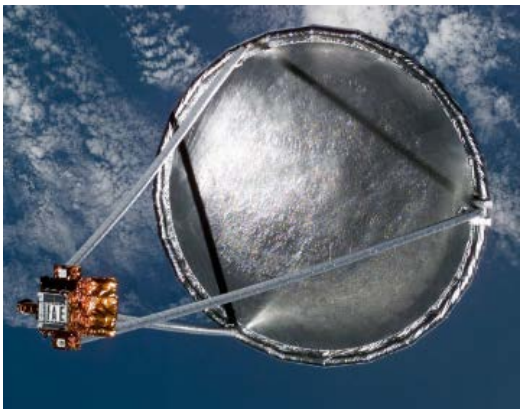

Figure 2. Inflatable Antenna Experiment [6]

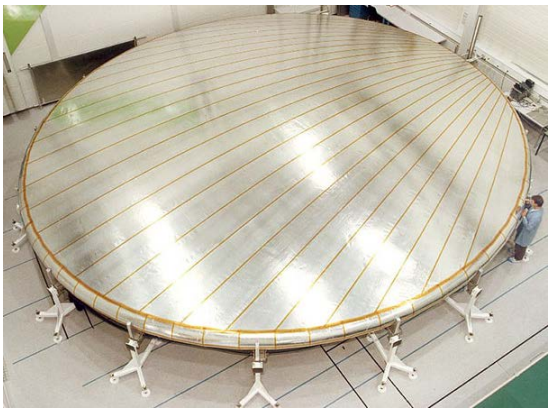

Figure 3. Contraves re-enforced antenna [7]

Previous work done by our group [9],[10] led to the development of a design methodology and a working prototype of an inflatable antenna. The antenna was built as an initially flat axisymmetric membrane unit inflated using gas from sublimation of chemical powder benzoic acid. A manufacturing methodology was developed and tested to incorporate UV curable resin ribs to provide stiffness to the membrane upon deployment. Prototype inflatable units have been built and developed. Studies and tests have shown the design to be feasible for producing required membrane tension. Our focus in the present paper is to identify the extent to which these units can be scaled up in size and complexity. This would be the next step in identifying required structural traits and sensitive design parameters.

## Methodology

This section discusses our methodology for characterising surface geometries of developed inflatable units. The structural response is simulated using non–linear finite element package LS-dyna. Surface precision is estimates based on Root Mean Square (RMS) error from an ideal paraboloid surface. We present our calculations for varying f/d ratios to understand feasible regions for antenna feed placement. We then go on to discuss the effect of scaling-up the structure on its attained shape and the feasibility of using multiple inflatables to enhance surface characteristics required for efficient reflectors.

**Structural response characterization**

A finite element model is setup to simulate Mylar membrane mechanics. The membrane was modelled as Mylar with a Young's modulus of 710,000 psi, density of 1,039 kg/m$^3$ and Poisson's ratio of 0.38. A thickness of 1mil or $2.54\times10^{-4}$ m was used. The inflation pressure was modelled as gas mass flow rate from 1.5 g of benzoic acid sublimate at varying temperatures. The goal of our analysis is to understand wrinkle formation on the inflatable membrane's surface and its final developed geometry.

**Expected radiative performance**

Structural simulations lead to an understanding of expected wrinkle free regions. In the case of axisymmetric membranes these can be demarcated into distinct regions [11]. To study the net deviation from a double curved parabola, the RMS error on the achieved surface was calculated as follows:

$$e_{ems} = \left( \int \left( \delta l / 2 \right)^2 dA / A \right)^{1/2} \tag{1}$$

Here $\delta l$ represents a change in path-length of electromagnetic radiation. In the case, where deviations from perfect paraboloid are small, the path length deviation may be approximated by the following formula:

$$\delta l = 2\Delta z \cos^2 \theta \tag{2}$$

Here $\Delta z$ represents the change in axial distance from the surface and $\theta$ represents the associated angle of meridian slope of the paraboloid. Deviations from perfect paraboloids led to loss of radiated power and have been characterized in terms of the rms error [12] as shown:

$$G / G_{ideal} = \exp\left( -\left( 4\pi e_{rms} / \lambda \right)^2 \right) \tag{3}$$

We look at errors over various *f/d* ratios to understand regions of the membrane's inflated surface. In the case of axisymmetric membranes, this region is expected to translate as a radial patch over the membrane's surface effectively like a 'parabolic cap' a [13] on top of the inflatable membrane.

**Concept inflatable assembly**

A method of effecting outward stretching at the membrane's circumference, we introduce the idea of membrane assemblies. Lowering f/d ratios cause greater influence of circumferential forces on the centre of the axisymmetric membrane. This leads to a 'flatter' and more parabolic membrane. We look into membrane unit assemblies that could help achieve this. Figure 4 shows a concept of an antenna system consisting of three inflatable units assembled together. These include a paraboloid element described earlier, a toroidal unit and a connecting membrane skin.

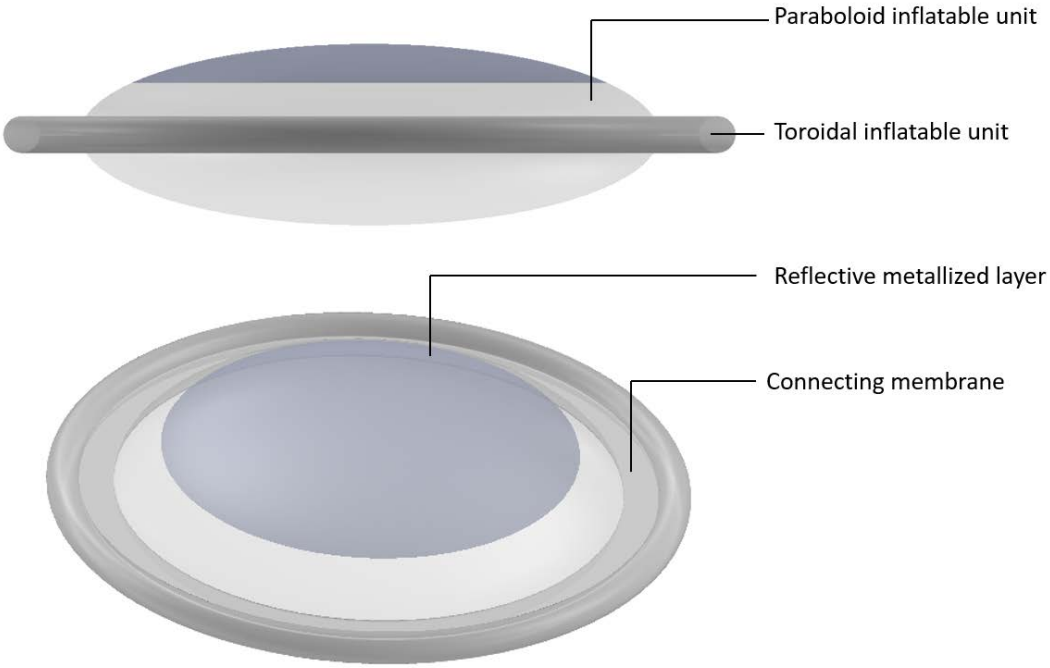


Figure 4. Inflatable reflector assembly concept

**Large scale structures**

Conducting full scale structural simulations on large inflatable assemblies is time intensive and not computationally efficient. An alternate strategy is to perform reduced order simulations using discretized approximation. As shown in Figure 5 , the discretized structure consists of a truss assembly also known as a voxel [14]. We use this method to understand general structural effects on varying geometry and size of inflatable structures. 6-DoF (Degree of Freedom) element stiffness matrices were computed for each element in the voxel as shown in (4).

$$K^e = R^{e^T} k^e \begin{bmatrix} 1 & -1 \\ -1 & 1 \end{bmatrix} R^e \tag{4}$$

Where $k^e$ represents the stiffness of each element and $R^e$ represents a transformation matrix given by:

$$R^e = \frac{1}{l^e} \begin{bmatrix} x_n^e & y_n^e & z_n^e & 0 & 0 & 0 \\ 0 & 0 & 0 & x_n^e & y_n^e & z_n^e \end{bmatrix} \tag{5}$$

Here $l$ represents the length of each element and $x$, $y$ and $z$ represent change in $x$ and $y$ and $z$ coordinated between adjacent elements in the voxel. The elemental stiffness matrices are scattered and summed to form the global stiffness matrix as follows:

$$K = \sum_e L^{e^T} K^e L^e$$

$L^e$ represents a binary matrix to scatter stiffness values over the length of the displacement vector. Nodal displacements are then found using the following equation:

$$d = K^{-1} F \tag{6}$$

## Results and discussion

The developed paraboloid inflatable unit has been subjected to inflation and rigidization tests in a vacuum chamber environment [10]. Figure 5a shows the developed shape of the prototyped unit inflated using chemical sublimate benzoic acid and rigidized using UV curable resins. Figure 5b and 5c show the developed deformations and stresses respectively corresponding to the same time frame as the experiment. It can be observed that wrinkles appear in high stress regions around the circumference of the inflatable. Wrinkles propagate across the circumferential direction but tend to dissipate as we move towards the centre of the axisymmetric unit. Based on observations, the inflatable's final shape can be divided into a wrinkle region, an intermediate region and a wrinkle free region. Measurements of the wrinkle free regions establish their feasibility of being used for high frequency Ka-band communication applications.

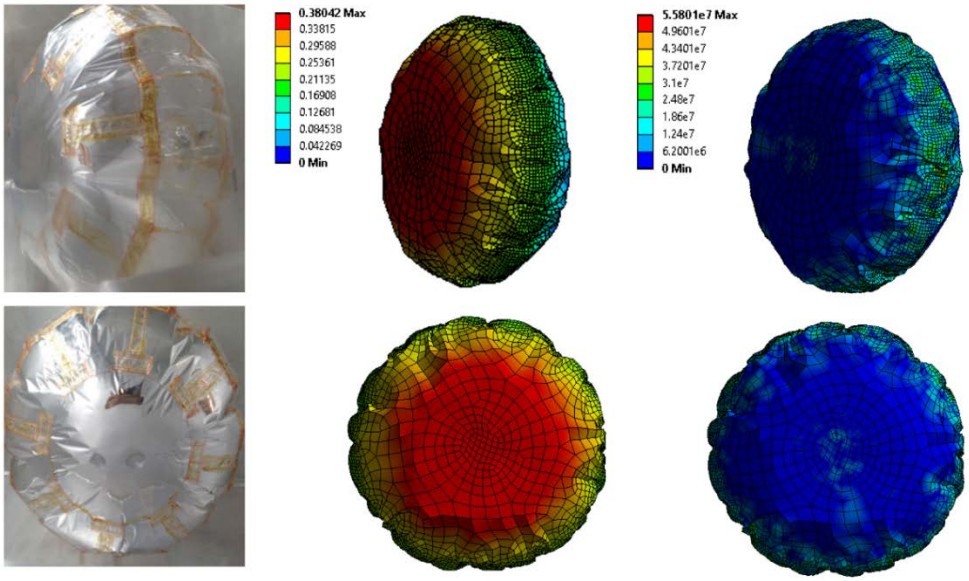


(a) (b) (c)

Figure 5. (a) Experiment images of final shape attained (b) Inflatable deformation plot (c) Inflatable equivalent stress plot

We repeated the above analysis for thermal cases likely encountered in Low Earth Orbits (LEO). The particular thermal load case was applied to simulate a circular LEO at an altitude of 370 km. Larger temperatures correspond to greater stresses due to larger sublimate pressures. This enhances the wrinkle-free region and reduces the amplitude of wrinkles formed at the circumference. On the other hand, low temperatures lead to loss in stiffness and highly unreliable shapes. This could be mitigated as long as the membrane is rigidized while it has adequate stiffness.

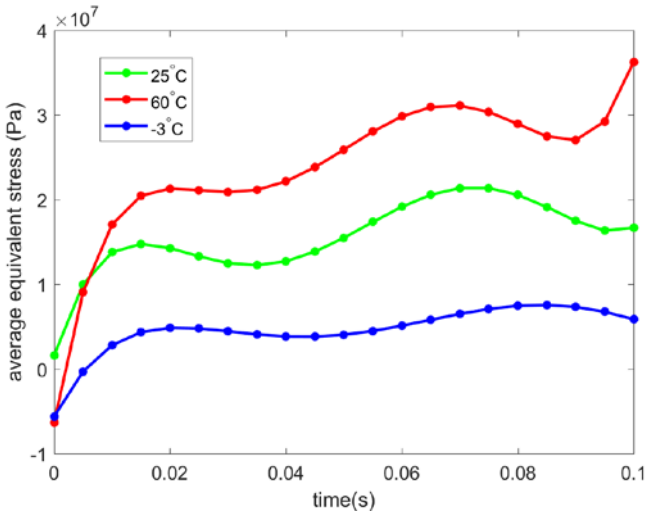


Figure 6. Stress development over hot and cold LEO regions

**Expected Ka band Gain Performance**

Obtained geometries from simulation were measured for their parabolicity. Geometric rms error calculated was used to determine expected gain relative to a perfect parabolic geometry. This calculation was repeated for parabola with varying f/d ratios and was carried out at Ka-band frequency of 27 Ghz.

Table 3. Geometric-shape errors

| f/d ratio | RMS error (mm) | Relative gain |
|---|---|---|
| 0.25 | 2.46 | 0.0004 |
| 0.50 | 1.23 | 0.1388 |
| 0.75 | 0.780 | 0.4520 |
| 1.0 | 0.506 | 0.7159 |

It can be observed that calculated errors have a strong bearing on gain relative to a perfect paraboloid. Further, it can be observed that the rms error tends to reduce for lower f/d ratios corresponding to a flatter reference parabola. This corresponds to the near flat wrinkle free central region as observed in experiments and simulations.

**Inflatable Concept - Structural Response**

Figure 7 shows developed deformations in a toroidal membrane unit as proposed. This unit shows a far more uniform strain distribution as compared to the other units. This points towards a more uniformly distributed stress decreasing the likelihood of wrinkle formation

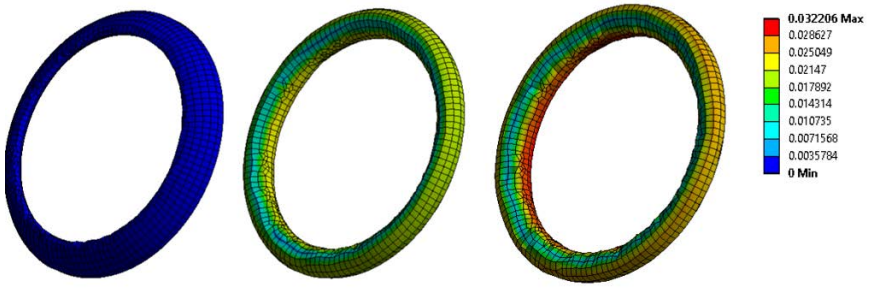


Figure 7. Stress development in toroidal inflatable unit

Figure 8 shows a comparison of maximum equivalent stresses generated in the previously described paraboloid membrane as compared to the proposed assembly. Based on the simulation results, we observe that the addition of a toroidal element considerably reduces stresses for the same amount of deformation. This could lead to lower stress concentrations and a more uniform parabolic surface. Further experimentation is needed to verify these results.

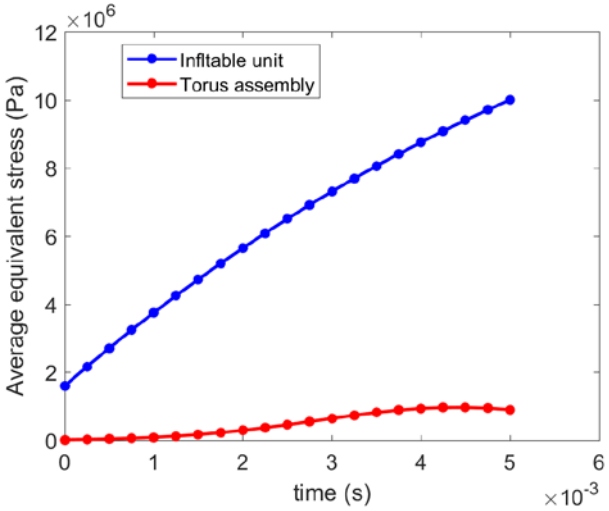


Figure 8. Comparison of equivalent stresses in a single unit and proposed assembly

## Conclusions and Future Work

Through this paper, we present a study that builds upon our previous work on inflatable reflectors. Finite element models of the previously developed design were developed to simulated their final inflated geometries. Stress distributions were plotted to understand local concentration and wrinkle formation tendencies. The obtained surface geometries were used to calculate root mean square errors relative to precise paraboloids. The error was then used to estimate a loss in gain and radiated power.

Basic shape analysis of developed inflatable prototypes shows that some regions of the inflatable can be utilized for high frequency communication at Ka-band and above. Thermo-structural analysis of the membrane's geometry suggests that 'over-pressurizing' the membrane could enhance available aperture area. This combined with a steerable feed could lead to a potent high-gain antenna at very low-cost, low-mass and low-volume.

Identified structural behaviour is used to propose a composite inflatable assembly concept. Preliminary analysis of the proposed composite inflatable assembly shows an order of magnitude reduction in stresses. This could lead to further enhancement of wrinkle free zones on axisymmetric membranes.

Further work needs to be done to validate simulation results for inflatable assemblies. A higher fidelity simulation model needs to be developed to capture dynamic behaviour if the membranes. An inverse model is required to understand optimum geometries that would lead to further stress distribution and improved shapes. Experimental prototypes are currently undergoing laser photogrammetry to accurately capture their material and dynamic behaviour. These results will be used to further refine the inflatable's design.

## References


[1] W. Lan, “CubeSat Design Standard Document.” .

[2] R. L. Staehle *et al.*, “Interplanetary CubeSats: Opening the Solar System to a Broad Community at Lower Cost,” p. 26.

[3] “Requirements, Design and Development of Large Space Antenna Structures,” Advisory Group for Aerospace Research and Development, 676, May 1980.

[4] R. E. Hodges, N. Chahat, D. J. Hoppe, and J. D. Vacchione, “A Deployable High-Gain Antenna Bound for Mars: Developing a new folded-panel reflectarray for the first CubeSat mission to Mars.,” *IEEE Antennas Propag. Mag.*, vol. 59, no. 2, pp. 39–49, Apr. 2017.

[5] I. I. Shapiro and H. M. Jones, “Perturbations of the Orbit of the Echo Balloon,” *Science*, vol. 132, no. 3438, pp. 1484–1486, 1960.

[6] R. E. Freeland and G. Bilyeu, “In-step inflatable antenna experiment,” *Acta Astronaut.*, vol. 30, pp. 29–40, Jul. 1993.

[7] Z.-Q. Liu, H. Qiu, X. Li, and S.-L. Yang, “Review of Large Spacecraft Deployable Membrane Antenna Structures,” *Chin. J. Mech. Eng.*, vol. 30, no. 6, pp. 1447–1459, Nov. 2017.

[8] C. H. M. Jenkins and G. Greschik, “Mechanics of Membrane Structures,” p. 62.

[9] A. Babuscia, T. Choi, and K.-M. Cheung, “Inflatable antenna for CubeSat: Extension of the previously developed S-Band design to the X-Band,” in *AIAA SPACE 2015 Conference and Exposition*, Pasadena, California, 2015.

[10] A. Babuscia, J. Sauder, A. Chandra, J. Thangavelautham, L. Feruglio, and N. Bienert, “Inflatable antenna for CubeSat: A new spherical design for increased X-band gain,” in *2017 IEEE Aerospace Conference*, 2017, pp. 1–10.

[11] G. Greschik, M. Mikulas, A. Palisoc, C. Cassapakis, and G. Veal, “Approximating paraboloids with axisymmetric pressurized membranes,” in *39th AIAA/ASME/ASCE/AHS/ASC Structures, Structural Dynamics, and Materials Conference and Exhibit*, Long Beach,CA,U.S.A., 1998.

[12] J. Ruze, “Antenna tolerance theory—A review,” *Proc. IEEE*, vol. 54, no. 4, pp. 633–640, Apr. 1966.

[13] G. Greschik, M. M. Mikulas, and A. Palisoc, “Torus-Less Inflated Membrane Reflector with an Exact Parabolic Center,” *AIAA J.*, vol. 42, no. 12, pp. 2579–2584, 2004.

[14] B. Jenett, C. Gregg, D. Cellucci, and K. Cheung, “Design of multifunctional hierarchical space structures,” in *2017 IEEE Aerospace Conference*, 2017, pp. 1–10.